Acknowledgement

This work was supported by the research grants from the Japanese Ministry of Health, Labour and Welfare (TI) and NIH grants GM-62134, and AI-068730 (JDL). The authors thank Cedric Francois and Paul Olson of Potentia Pharmaceuticals Inc., for providing us the GM grade compstatin.

References

Ambati, J., Anand, A., Fernandez, S., Sakurai, E., Lynn, B. C., Kuziel, W. A., Rollins, B. J., Ambati, B. K. (2003) An animal model of age-related macular degeneration in senescent Ccl-2- or Ccr-2-deficient mice. Nat. Med. 9,1390-1397.

Dewan A., Liu, M., Hartman, S., Zhang, S. S., Liu, D. T., Zhao, C., Tam, P. O., Chan, W. M., Lam, D. S., Snyder, M., Barnstable, C., Pang, C. P., Hoh, J. (2006) HTRA1 promoter polymorphism in wet age-related macular degeneration. Science 314,989-992.

Edwards, A. O., Ritter, R. 3rd., Abel, K. J., Manning, A., Panhuysen, C., Farrer, L. A. (2005) Complement factor H polymorphism and age-related macular degeneration. Science 308,421-424.

El-Mofty A., Gouras, P., Eisner, G., Balazs, E. A. (1978) Macular degeneration in rhesus monkey (Macaca mulatta). Exp. Eye Res. 27,499-502.

Gold, B., Merriam, J. E., Zernant, J., Hancox, L. S., Taiber, A. J., Gehrs, K., Cramer, K., Neel, J., Bergeron, J., Barile, G. R., Smith, R. T. (2006) AMD Genetics Clinical Study Group; G. S. Hageman, M. Dean, R. Allikmets. Variation in factor B (BF) and complement component 2 (C2) genes is associated with age-related macular degeneration. Nat. Genet. 38,458-462.

Goto, A., Akahori, M., Okamoto, H., Minami, M., Terauchi, N., Haruhata, Y., Obazawa, M., Noda, T., Honda, M., Mizota, A., Tanaka, M., Hayashi, T., Tanito, M., Ogata, N., and Iwata, T. (2009) Genetic Analysis of Typical Wet-Type Age-Related Macular Degeneration and Polypoidal Choroidal Vasculopathy in Japanese Population. J Biochem Dis Inform (in press).

Gotoh, N., Yamada, R., Hiratani, H., Renault, V., Kuroiwa, S., Monet, M., Toyoda, S., Chida, S., Mandai, M., Otani, A., Yoshimura, N., Matsuda, F. (2006) No association between complement factor H gene polymorphism and exudative age-related macular degeneration in Japanese. Hum. Genet. 120,139-143.

Hageman, G. S., Anderson, D. H., Johnson, L. V., Hancox, L. S., Taiber, A. J., Hardisty, L. I., Hageman, J. L., Stockman, H. A., Borchardt, J. D., Gehrs, K. M., Smith, R. J., Silvestri, G., Russell, S. R., Klaver, C. C., Barbazetto, I., Chang, S., Yannuzzi, L. A., Barile, G. R., Merriam, J. C., Smith, R. T., Olsh, A. K., Bergeron, J., Zernant, J., Merriam, J. E., Gold, B., Dean, M., Allikmets, R. (2005) A common haplotype in the complement regulatory gene factor H (HF1/CFH) predisposes individuals to age-related macular degeneration. Proc. Natl. Acad. Sci. U S A 102,7227-7232.

Haines, J. L., Hauser, M. A., Schmidt, S., Scott, W. K., Olson, L. M., Gallins, P., Spencer, K. L., Kwan, S. Y., Noureddine, M., Gilbert, J. R., Schnetz-Boutaud, N., Agarwal, A., Postel, E. A., Pericak-Vance, M. A. (2005) Complement factor H variant increases the risk of age-related macular degeneration. Science 308,419-421.

Iyengar, S. K., Song, D., Klein, B. E., Klein, R., Schick, J. H., Humphrey, J., Millard, C., Liptak, R., Russo, K., Jun, G., Lee, K. E., Fijal, B., Elston, R. C. (2004) Dissection of genomewide-scan data in extended families reveals a major locus and oligogenic susceptibility for age-related macular degeneration. Am. J. Hum. Genet.

74,20-39.

Klein, R. J., Zeiss, C., Chew, E. Y., Tsai, J. Y., Sackler, R. S., Haynes, C., Henning, A. K., SanGiovanni, J. P., Mane, S. M., Mayne, S. T., Bracken, M. B., Ferris, F. L., Ott, J., Barnstable, C., Hoh, J. (2005) Complement factor H polymorphism in age-related macular degeneration. Science 308,385-389.

Katragadda,M., Magotti,P., Sfyroera,G. and Lambris,J.D. (2006). Hydrophobic effect and hydrogen bonds account for the improved activity of a complement inhibitor, compstatin. *J. Med. Chem.*, 49, 4616-4622

Majewski, J., Schultz, D. W., Weleber, R. G., Schain, M. B., Edwards, A. O., Matise, T. C., Acott, T. S., Ott, J., Klein, M. L. (2003) Age-related macular degeneration--a genome scan in extended families. Am. J. Hum. Genet. 73,540-550.

Mullins, R. F., Russell, S. R., Anderson, D. H., Hageman, G. S. (2000) Drusen associated with aging and age-related macular degeneration contain proteins common to extracellular deposits associated with atherosclerosis, elastosis, amyloidosis, and dense deposit disease. FASEB J 14,835-846.

Nicolas, M. G., Fujiki, K., Murayama, K., Suzuki, M. T., Mineki, R., Hayakawa, M., Yoshikawa, Y., Cho, F., Kanai, A. (1996) Studies on the mechanism of early onset macular degeneration in cynomolgus (Macaca fascicularis) monkeys. I. Abnormal concentrations of two proteins in the retina. Exp. Eye Res. 62,211-219.

Nicolas, M. G., Fujiki, K., Murayama, K., Suzuki, M. T., Shindo, N., Hotta, Y., Iwata, F., Fujimura, T., Yoshikawa, Y., Cho, F., Kanai, (1996) A. Studies on the mechanism of early onset macular degeneration in cynomolgus monkeys. II. Suppression of metallothionein synthesis in the retina in oxidative stress. Exp. Eye Res. 62,399-408.

Okamoto, H., Umeda, S., Obazawa, M., Minami, M., Noda, T., Mizota, A., Honda, M., Tanaka, M., Koyama, R., Takagi, I., Sakamoto, Y., Saito, Y., Miyake, Y., Iwata, T. (2006) Complement factor H polymorphisms in Japanese population with age-related macular degeneration. Mol. Vis. 12,156-158.

Russell, S. R., Mullins, R. F., Schneider, B. L., Hageman, G. S. (2000) Location, substructure, and composition of basal laminar drusen compared with drusen associated with aging and age-related macular degeneration. Am J Ophthalmol 129,205-214.

Schick, J. H., Iyengar, S. K., Klein, B. E., Klein, R., Reading, K., Liptak, R., Millard, C., Lee, K. E., Tomany, S. C., Moore, E. L., Fijal, B. A., Elston, R. C. (2003) A whole-genome screen of a quantitative trait of age-related maculopathy in sibships from the Beaver Dam Eye Study. Am. J. Hum. Genet. 72,1412-1424.

Stafford, T. J., Anness, S. H., Fine, B. S. (1984) Spontaneous degenerative maculopathy in the monkey. Ophthalmology 91,513-521.

Suzuki MT, Terao K, Yoshikawa Y. (2003) Familial early onset macular degeneration in cynomolgus monkeys (Macaca fascicularis). Primates. 44,291-294.

Umeda, S., Ayyagari, R., Allikmets, R., Suzuki, M. T., Karoukis, A. J., Ambasudhan, R., Zernant, J., Okamoto, H., Ono, F., Terao, K., Mizota, A., Yoshikawa, Y., Tanaka, Y., Iwata, T. (2005) Early-onset macular degeneration with drusen in a cynomolgus monkey (Macaca fascicularis) pedigree: exclusion of 13 candidate genes and loci. Invest. Ophthalmol. Vis. Sci. 46,683-691.

Umeda, S., Suzuki, M. T., Okamoto, H., Ono, F., Mizota, A., Terao, K., Yoshikawa,

Y., Tanaka, Y., Iwata, T. (2005) Molecular composition of drusen and possible involvement of anti-retinal autoimmunity in two different forms of macular degeneration in cynomolgus monkey (Macaca fascicularis). FASEB J. 19,1683-1685.

Yates, J.R.W., Sepp T, Matharu, B.K., Khan, J.C., Thurlby, D.A., Shahid, H., Clayton, D.G., Hayward, C., Morgan, J., Wright, A.F.,Ph.D., Armbrecht, A.M., Dhillon, B., Deary, I.J., Redmond, E., Bird, A.C., and Moore, A.T. Complement C3 Variant and the Risk of Age-Related Macular Degeneration. N Engl J Med. 357,553-561.

Yang, Z., Camp, N. J., Sun, H., Tong, Z., Gibbs, D., Cameron, D. J., Chen, H., Zhao, Y., Pearson, E., Li, X., Chien, J., Dewan, A., Harmon, J., Bernstein, P. S., Shridhar, V., Zabriskie, N. A., Hoh, J., Howes, K., Zhang, K.. (2006) A variant of the HTRA1 gene increases susceptibility to age-related macular degeneration. Science. 314,992-993.

Yoshida, T., Wan, A.D., Zhang, H., Sakamoto, R., Okamoto, H., Minami, M., Obazawa, M., Mizota, A., Tanaka, M., Saito, Y., Takagi, I., Hoh, J., and Iwata, T. (2007) HTRA1 Promoter Polymorphism Predisposes Japanese to AMD. Mol Vis 13,545-548.

Exp. Anim. 59(2), 171–182, 2010

—Original—

Comparative Proteomic Analyses of Macular and Peripheral Retina of Cynomolgus Monkeys (*Macaca fascicularis*)

Haru OKAMOTO[1,2], Shinsuke UMEDA[1], Takehiro NOZAWA[3], Michihiro T. SUZUKI[4], Yasuhiro YOSHIKAWA[5], Etsuko T. MATSUURA[6], and Takeshi IWATA[1]

[1]*Division of Molecular & Cellular Biology, National Institute of Sensory Organs, National Hospital Organization Tokyo Medical Center, 2–5–1 Higashigaoka, Meguro-ku, Tokyo 152-8902, Japan,* [2]*Department of Advanced Biosciences, Ochanomizu University, 2–1–1 Otsuka, Bunkyo-ku, Tokyo 112-8610, Japan,* [3]*Analytical Instrument Division, AMR Inc., 2–13–18 Nakane, Meguro-ku, Tokyo 152-0031, Japan,* [4]*The Corporation for Production and Research of Laboratory Primates, 1–1 Hachimandai, Tsukuba-shi, Ibaraki 305-0843, Japan,* [5]*Department of Biomedical Science, Graduate School of Agricultural and Life Sciences, The University of Tokyo, 1–1–1 Yayoi, Bunkyo-ku, Tokyo 113-8657, Japan, and* [6]*The Natural/Applied Sciences Division, Ochanomizu University, 2–1–1 Otsuka, Bunkyo-ku, Tokyo 112-8610, Japan*

Abstract: The central region of the primate retina is called the macula. The fovea is located at the center of the macula, where the photoreceptors are concentrated to create a neural network adapted for high visual acuity. Damage to the fovea, e.g., by macular dystrophies and age-related macular degeneration, can reduce central visual acuity. The molecular mechanisms leading to these diseases are most likely dependent on the proteins in the macula which differ from those in the peripheral retina in expression level. To investigate whether the distribution of proteins in the macula is different from the peripheral retina, proteomic analyses of tissues from these two regions of cynomolgus monkeys were compared. Two-dimensional gel electrophoresis and mass spectrometry identified 26 proteins that were present only in the macular gel spots. The expression levels of five proteins, cone photoreceptor specific arrestin-C, γ-synuclein, epidermal fatty acid binding protein, tropomyosin 1α chain, and heterogeneous nuclear ribonucleoproteins A2/B1, were significantly higher in the macula than in the peripheral retina. Immunostaining of macula sections by antibodies to each identified protein revealed unique localization in the retina, retinal pigment epithelial cells and the choroidal layer. Some of these proteins were located in cells with higher densities in the macula. We suggest that it will be important to study these proteins to determine their contribution to the pathogenesis and progression of macula diseases.

Key words: 2D-gel electrophoresis, macula, mass spectrometry, retina

(Received 16 September 2009 / Accepted 13 November 2009)

Address corresponding: T. Iwata, Division of Molecular & Cellular Biology, National Institute of Sensory Organs, National Hospital Organization Tokyo Medical Center, 2–5–1 Higashigaoka, Meguro-ku, Tokyo 152-8902, Japan

Introduction

The macula is an oval-shaped, highly pigmented spot near the central region of the primate retina. It is approximately 2.0 mm in diameter in humans [31] and 1.0 mm in macaque monkeys [36–38]. The fovea is located at the center of macula where the retinal thickness is reduced to approximately 0.1 mm and consists of only the retinal pigment epithelium (RPE), photoreceptor layer, external limiting membrane, outer nuclear layer, outer plexiform layer, and inner limiting membrane [30]. The cone density in the foveal pit is the highest in the retina, and rods, retinal ganglion cells (RGCs), and blood vessels are not present. These cones are connected to large numbers of RGCs, which are highly dense at the parafovea [31]. The cone-dense fovea mediates high-acuity central vision, and any damage to the macula can lead to severely depressed central visual acuity as observed in patients with macular dystrophies and age-related macular degeneration (AMD).

Because of the unique cellular organization of the macula, investigators have performed comprehensive gene expression studies of the macula and peripheral retina using DNA microarray analysis or Serial Analysis of Gene Expression (SAGE). Sharon *et al.* used SAGE to show that several genes are preferentially expressed in the human macula and RPE. Most of these genes are associated with the function of the RGCs, and were presumably detected because of the high density of RGCs in the macula [35]. Bowes Rickman *et al.* also performed SAGE on human retinas and isolated RPE cells and identified genes that are abundantly expressed in cones, RGCs, and RPE cells [3]. Ishibashi *et al.* performed 4 K DNA microarray analysis on RPE cells from the macula and reported five differentially expressed genes which were confirmed by real-time PCR [18]. Recently, Radeke *et al.* [32] and van Soest *et al.* [48] used 22 K DNA microarray analyses and identified a number of genes that were differentially expressed in the macula and peripheral retina. In each study, five of these genes were found to be highly expressed in RPE cells in the macula. van Soest *et al.* showed by immunohistochemistry that the WAP four-disulfide core domain 1, one of the highly expressed proteins, is present in the RPE cells in the macula. However, the expression level of the mRNAs does not always correlate with the expression levels of the proteins.

Recent technical advances in proteomics allow the direct determination of the protein profile of body fluids and tissue homogenates. Proteomic analyses of the retina were first performed by Nishizawa *et al.* [28], and several groups have catalogued the retinal proteins using single or two-dimensional (2D) gel electrophoresis followed by mass spectrometry (MS) analysis [1, 5, 50]. Ethen *et al.* examined cadaver eyes with AMD by proteomic analyses and reported that the expression of proteins changed with the progression of AMD, and the changes in the macula were different from those in the peripheral retina [10]. These findings indicate that the macular region of the retina is different from the peripheral retina not only in its morphology but also in its protein content.

Proteomic studies of the macula are difficult to perform because of the lack of fresh human eyes, and small sample size of the macula. To overcome these problems, we selected non-human primate eyes of the cynomolgus monkey (*Macaca fascicularis*). The retina and visual system of macaque monkeys are quite similar to those of humans [14, 29], and monkeys with characteristics of macular diseases have been reported by many investigators [9, 16, 19, 25, 39, 40] as well as our previous studies [26, 27, 44–47]. Thus, the purpose of this study was to identify proteins present at high levels in the macula to better understand the biology of this unique tissue. To accomplish this task, we performed proteomic analyses on retinal tissues obtained from the macular region and the periphery for comparison.

Materials and Methods

Preparation of cynomolgus monkey eyes

All experiments on monkeys were approved by the Animal Ethics Committee of the Tsukuba Primate Research Center (TPRC) and were conducted in accordance with The Association for Research in Vision and Ophthalmology Statement for the Use of Animals in Ophthalmic and Vision Research. Eight eyes from eight normal female cynomolgus monkeys (*Macaca fascicularis*) whose ages ranged between 13 to 19 years were studied. Eyes were removed approximately one hour

after death and treated with RNAlater (Applied Biosystems, Tokyo, Japan). Other tissues from these animals were used by other research groups at the TPRC. Three-millimeter-diameter pieces of macular and peripheral retina containing neural retina, RPE and choroidal layer were punched out and frozen until use. The proteins extracted from the tissues of eight eyes were pooled for the analyses.

Protein extraction and 2D-gel electrophoresis

The proteins from the macula and peripheral retina were extracted after homogenization and sonication in sample buffer [7 M urea, 2 M thiourea, 4% CHAPS, 50 mM DTT, 40 mM Tris, 0.2% Bio-Lyte 3/10 (Bio-Rad, Hercules, CA, USA)]. After centrifugation for 15 min × 3 at 14,000 rpm (20,800 × *g*), the supernatant was collected. The lysate was precipitated using Ready Prep 2D cleanup kit (Bio-Rad) and redissolved in sample buffer. The protein concentration was determined with the RC-DC protein assay kit (Bio-Rad) according to the manufacturer's instruction. Protein samples (300 μg) were separated by isoelectric focusing (IEF) using 17-cm immobilized pH gradient (IPG) strips. After 12 to 16 h of rehydration at 20°C, the IEF sample was used for the first dimension with an initial voltage of 250 V for 15 min and then increased to 10,000 V for 3 h and held until 60,000 V-h was reached. Immediately after the IEF, the IPG strips were stored at –20°C until the equilibration step was carried out. The IPG strips were equilibrated for 20 min in buffer containing 6 M urea, 2% SDS, 0.375 M Tris (pH 8.8), and 20% glycerol under reduced conditions with 2% DTT, followed by another incubation for 10 min in the same buffer under alkylating conditions with 2.5% iodoacetamide. The equilibrated IPG strips were electrophoresed for the second dimension using 12% acrylamide gels. Two dimensional gel electrophoresis was performed at four different pH ranges, viz., pH 3–10, 4–7, 5–8, and 7–10. After the 2D gel electrophoresis, the proteins were stained with SYPRO Ruby (Bio-Rad). The images for the macula and peripheral retina were compared with ImageMaster 2D Platinum ver.5.0 (GE Healthcare Bio-Sciences, Piscataway, NJ, USA) followed by visual inspection. The gel spots numbered in Fig. 1 were excised. Two dimensional gels of peripheral retina were stained with Bio-safe Coomassie (Bio-Rad). Then, 46 spots from the Coomassie-stained gel were excised (Fig. 1, Peripheral Coomassie).

In gel digestion and LC-MS/MS analyses

Each gel piece was cut into approximately one cubic millimeter and washed twice with 50 mM ammonium bicarbonate/50% acetonitrile. After destaining, the gel pieces were rinsed with distilled water, and incubated with acetonitrile for 20 min. The supernatant was discarded and the gel pieces were completely dried before incubation with 10 mM DTT in 100 mM ammonium bicarbonate for 45 min at 56°C. The supernatant was discarded and the pieces were incubated in the dark with 55 mM iodoacetamide in 100 mM ammonium bicarbonate (30 min, at room temperature). The supernatant was discarded, and the gels were washed three times. Finally, the gel pieces were completely dried before tryptic digestion in sequencing grade trypsin solution (12.5 ng/μl; Promega, Madison, WI, USA) in 50 mM ammonium bicarbonate. The digestion was performed at 37°C overnight, and the extraction step was performed once with 25 mM ammonium bicarbonate, twice with 5% formic acid, and finally with distilled water. The extracted peptides were pooled and dried. After re-suspending in 40 μl of aqueous 0.01% trifluoroacetic acid/2% acetonitrile, the samples were analyzed by LC (liquid chromatography)-MS/MS. LC-MS/MS was performed with a combined Paradigm MS4 (Michrom BioResources, Auburn, CA, USA) and an ESI mass spectrometer (LCQ Deca XP plus or Finnigan LTQ, Thermo Fisher Scientific, Yokohama, Japan; assembled by AMR Inc., Tokyo, Japan). For the LCQ analysis, sample peptides were separated in nano column (AMR Inc.) with solvent A (2% acetonitrile/0.1% formic acid) and B (90% acetonitrile/0.1% formic acid) at flow rate of 0.6 μl/min, gradient of 5 to 95% solvent B over 40 min. For the LTQ analysis, peptides were separated on Magic C18 (Michrom BioResources) with solvent A and B, a flow rate 1.5 μl/min, gradient of 5 to 95% solvent B over 30 min. The identification of the proteins from the MS/MS spectra was performed using protein identification software (Bioworks ver.3.1, Thermo Fisher Scientific) and UniProtKB/Swiss-Prot database (Release 48.8) which was preliminarily extracted by the species "human" (13,361 entries). Peak list generation and database searches were performed with the following

parameters: mass tolerance for precursor ions, 2.5 amu; mass tolerance for fragment ions, 0.00 amu; enzymatic cleavage position, after lysine or arginine; number of missed cleavage sites permitted, 2; fixed modification, carbamide-methylation (+57.02 Da) for cysteine; variable modification, oxidation (+16 Da) for methionine. The peptide sequences were filtered by delta Cn score and peptide Cross Correlation (XC) score. The threshold level of delta Cn scores was >0.1 for peptide sequences from both measurement devices. The threshold levels of XC scores for each charge (+1/+2/+3) were >1.5/2.0/3.7 for LCQ and >1.9/2.2/3.7 for LTQ. Then, the correlations between the observed in gel images and the theoretical molecular weight and pI were considered. When peptides matched multiple members of the protein family, the protein which had the most number of peptides that matched the amino acid sequence was selected. In case of equal numbers, both proteins were listed.

Western blotting and immunohistochemical analysis of macula

Five to fifteen micrograms of macula or peripheral retinal homogenates were diluted in a double volume of SDS buffer and separated by 1D-PAGE followed by transfer to PVDF (polyvinylidene difluoride) membrane. Membranes were blocked with blocking solution (Blocking Solution Concentrate, KPL, Gaithersburg, MD, USA), skim milk, or BSA dissolved in PBS and probed with one of the following primary antibodies (Abs): chicken Ab to human arrestin-C (GenWay Biotech, San Diego, CA, USA), rabbit Ab to human synuclein gamma (Novus Biologicals, Littleton, CO, USA), rat Ab to human epidermal fatty acid binding protein (E-FABP) (R&D Systems, Minneapolis, MN, USA), rabbit Ab to tropomyosin Br-1, Br-3 (CHEMICON International, Temecula, CA, USA), mouse Ab to chicken tropomyosin TM311 (Abcam, Cambridge, UK), and goat Ab to human heterogeneous nuclear ribonucleoproteins (hnRNPs) A2/B1 (Santa Cruz Biotechnology, Santa Cruz, CA, USA). The specific signals were detected with one of the following secondary antibodies: horseradish peroxidase (HRP)-conjugated goat Ab to mouse IgG (Jackson ImmunoResearch Laboratories, West Grove, PA, USA), HRP-conjugated goat Ab to rabbit IgG (Pierce, Rockford, IL, USA), HRP-conjugated rabbit Ab to chicken/turkey IgG (Zymed Laboratories, South San Francisco, CA, USA), HRP-conjugated donkey Ab to goat IgG (Jackson ImmunoResearch Laboratories), HRP-conjugated goat Ab to rat IgG (Zymed Laboratories). The signals were made visible by chemiluminescence reactions and examined with a chemiluminescence imager (Lumi-Imager F1; Roche Diagnostics, Tokyo, Japan). An enucleated eye from a normal female cynomolgus monkey (age 13 years) was fixed in 10% neutralized and buffered formaldehyde solution at 4°C overnight and then dehydrated. The specimens were embedded in paraffin and serially sectioned at 4 μm thickness. The specimens were treated for antigen retrieval by autoclaving in Target Retrieval Solution (Dako, Carpinteria, CA, USA) for 20 min at 121°C. The sections were then blocked with Dako Protein Block (Dako) or skim milk or BSA in PBS. The primary antibodies were the same as used for the western blotting, and rabbit Ab to human platelet/endothelial cell adhesion molecule (PECAM1) (Proteintech Grroup, Chicago, IL, USA). For signal detection after rinsing off the primary antibodies, the sections were incubated with one of following secondary antibodies: Alexa 488-conjugated goat Ab to anti-mouse IgG, Alexa 568-conjugated goat Ab to anti-mouse IgG, Alexa 488-conjugated goat Ab to anti-rabbit IgG, Alexa 568-conjugated goat Ab to anti-rabbit IgG, Alexa 488-conjugated donkey Ab to anti-goat IgG, Alexa 568-conjugated goat Ab to anti-chicken IgG, and Alexa 488-conjugated goat Ab to anti-rat IgG (all secondary antibodies from Invitrogen, Tokyo, Japan). After rinsing off the antibodies, the sections were examined by confocal laser scanning microscope (Radiance 2100, Bio-Rad). The cell nuclei were stained with DAPI (4',6-diamino-2-phenylindole). To determine the location of the signals, one of the sections was stained with hematoxylin and eosin.

Results

Identification of macula enriched proteins

Approximately 700 spots were detected in the macular and peripheral retinal tissues in the 2D gel stained with SYPRO Ruby (pH range 3–10; Fig. 1A). Sixty percent of these spots were found in both samples. Butt *et al.* have described the difficulties of IEF separation by RNAlater contaminations [4]. Our samples were de-

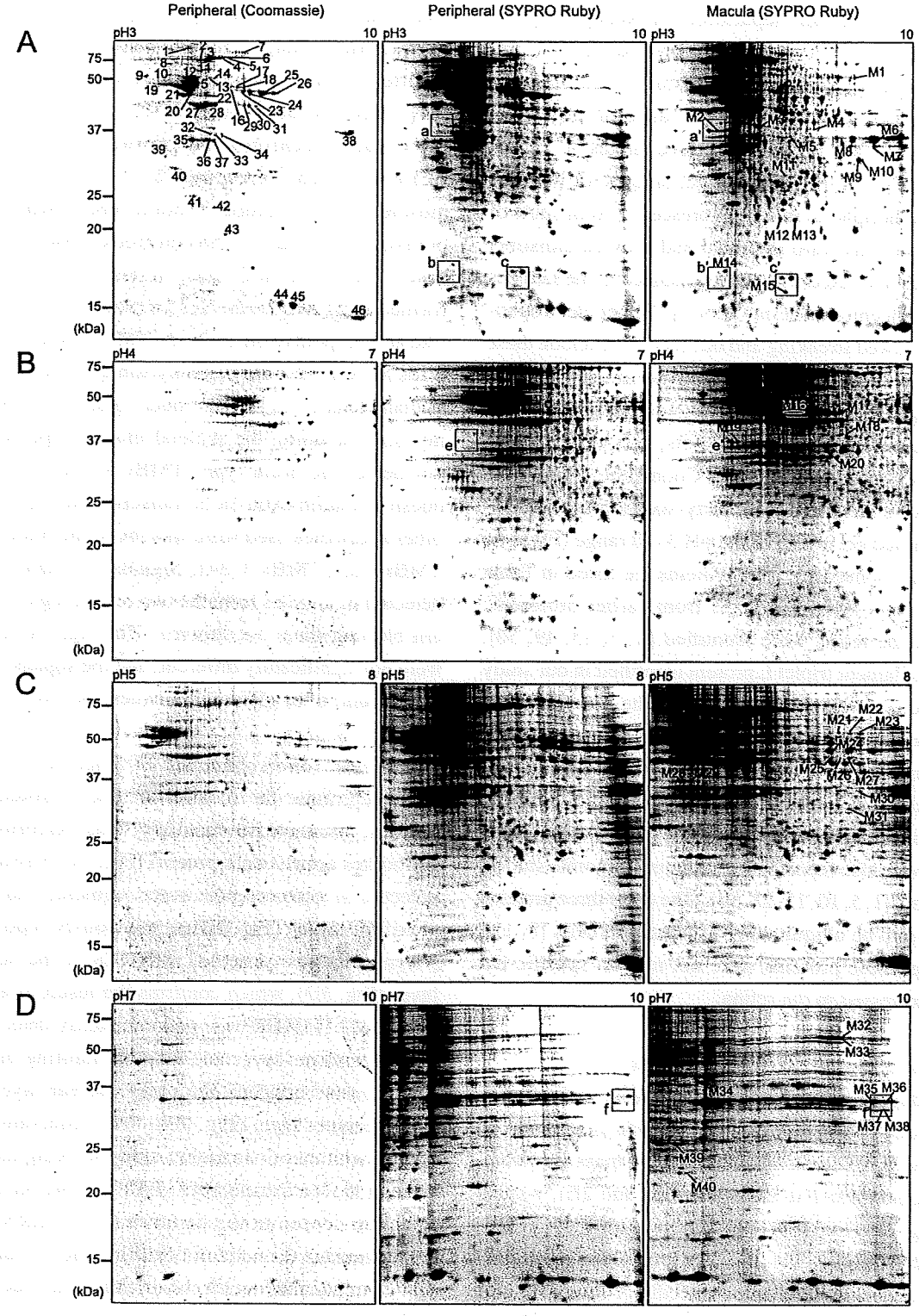

Fig. 1. Separation of monkey retina proteins on 2D gels. Proteins extracted from the peripheral retina and macula (300 μg each) were isoelectric focused at four different pH ranges; pH 3–10 (A), 4–7 (B), 5–8 (C), 7–10 (D). Then the IPG strips were separated on 12% SDS-page gels and stained by SYPRO Ruby. Forty spots marked by spot IDs were unique to the macula gel images and identified by LC-MS/MS. Boxed areas (a–f, Peripheral-SYPRO Ruby; a'–f', Macula-SYPRO Ruby) correspond to the enlarged images in Fig. 2. Two dimensional gels of peripheral retina were also stained by Bio-safe Coomassie. Forty-six spots marked by spot number were identified by LC-MS/MS.

salted prior to the IEF separation by Ready Prep 2D cleanup kit using TCA (trichloroacetic acid) acetone precipitation which resulted in successful separations. To obtain a further separation, the pH range of the 2D gel electrophoresis was narrowed to three ranges; 4–7, 5–8, and 7–10 (Fig. 1B–D). Among gel images for both the macula and peripheral retina, fluorescence from spots of abundant proteins were saturated and showed indistinct spot boundaries. Excess proteins contained in the samples were not concentrated at one spot by 2D gel electrophoresis and showed streaking and outliers. To exclude these proteins which were identified from seemingly macular specific spots, abundant proteins were identified. To clarify the outline of saturated spots, gels of peripheral retina were stained with Bio-safe Coomassie. Forty-nine proteins were identified from forty-six spots in the Coomassie stained gel image of the pH 3–10 range (Fig. 1A, Peripheral Coomassie). The proteins are listed in Table 1. Forty-eight known proteins from earlier proteomic studies of the retina were identified [1, 5, 15, 49, 50]. The neurofilament triplet L protein identified in our study has not been previously identified by the proteomic approach but it has been reported in a SAGE analysis [35]. The 49 proteins were expressed in both the macula and peripheral retina, while 26 proteins were identified from 40 spots in macula gel images (Table 2). Twenty-three of these were also reported in previous proteomic studies of the retina [1, 5, 10, 15, 22, 50]. The other three proteins are known to be ubiquitously expressed in cells [8, 11]. Therefore, these proteins were not macula specific but widely expressed in the retina.

Validation of macula enriched proteins

To obtain the relative expression levels of the identified proteins, western blot analysis was performed on the following five proteins identified by mass spectrometry: tropomyosin 1 α chain (Fig. 2A and 2E), γ-synuclein (Fig. 2B), E-FABP (Fig. 2C), arrestin-C (Fig. 2D), and hnRNPs A2/B1 (Fig. 2F). Arrestin-C has been identified as a cone photoreceptor-specific protein [33], and thus served as a positive control for this study. γ-Synuclein is a protein known to be up-regulated in cancer cells [20]. hnRNPs A2/B1 is also known to be up-regulated in carcinoma cells [42]. E-FABP is a reactive lipid scavenger [2]. Four proteins, including arrestin-C, were confirmed to have higher expression in the macula by western blotting. Tropomyosin 1 α chain has been reported to have many isoforms by alternative splicing [34]. MS/MS data from spot M2 (Fig.1A, Macula SYPRO Ruby) identified the peptide sequence CAELEEELK, which corresponded to isoform 1 (skeletal muscle type) or isoform 5 (brain type, TMBr-3) of tropomyosin 1 α chain in the UniProtKB/Swiss-Prot database. Based on these data, western blotting was performed using two antibodies for tropomyosin 1 α chain. The anti-tropomyosin antibody TM311 detects 19 amino acids in exon 1a of the tropomyosin gene family in mammalian tissues, viz., alpha-, beta-, gamma-, delta- tropomyosin, including the skeletal muscle type but it does not detect the brain type (TMBr-3), because TMBr-3 doesn't contain exon 1a in transcription sequence. The other antibodies used were specific to the brain isoforms TMBr-1 and TMBr-3 [34]. Signals of TMBr-1 were not detected in samples from the two retinal regions by western blotting (data not shown). The signals of TMBr-3 were not significantly different, and the signals to TM311 were found to be different between the two regions.

Tissue localization of macula enriched proteins

To determine the location of the 5 proteins in the macula, immunohistochemistry was performed using antibodies against each protein (Fig. 3). Arrestin-C was detected in photoreceptor outer segments and the outer plexiform layer (Fig. 3B) as previously reported [33]. γ-Synuclein was detected in RGCs in the nerve fiber layer (Fig. 3D), which confirms the result of a previous study [43]. E-FABP was predominantly detected in the outer plexiform layer and external limiting membrane, which exists between the outer nuclear layer and the photoreceptor layer (Fig. 3G). Our observation is consistent with that of an earlier study by Kingma *et al.* reporting the localization of E-FABP to Müller cells [21], which are dense in the parafovea [7]. hnRNPs A2/B1 was located in the nucleus of cells in the retinal ganglion cell layer, the inner nuclear layer, the outer nuclear layer, and the RPE with different intensities (Fig. 3E). TM311 was detected in the choroidal layer (Fig. 3F), while tropomyosin Br-3 was located in photoreceptor inner segments and the outer plexiform layer (Fig. 3C). To determine the localization of tropomyosin detected by TM311

Table 1. Proteins identified in 46 spots of Coomassie-stained gel

Spot No.[a]	Protein name	Database accession No.[b]	MW (kDa)[c]	pI[c]	Sequence coverage (%)	No. of peptide
1	Heat shock protein HSP 90-alpha	P07900	84.5	4.94	10.53	7
1	Heat shock protein HSP 90-beta	P08238	83.1	4.97	6.09	4
2	Heat shock cognate 71 kDa protein	P11142	70.9	5.37	29.41	17
2	Vacuolar ATP synthase catalytic subunit A, ubiquitous isoform	P38606	68.3	5.35	20.75	10
2	Lamin B2	Q03252	67.7	5.29	17.67	9
2	Heat shock 70 kDa protein 1	P08107	70.1	5.48	16.54	9
2	Stress-70 protein, mitochondrial	P38646	73.7	5.87	9.57	5
3	Stress-70 protein, mitochondrial	P38646	73.7	5.87	8.25	4
3	Serum albumin	P02768	69.4	5.92	6.9	4
4	Serum albumin	P02768	69.4	5.92	6.9	3
5	Serum albumin	P02768	69.4	5.92	7.39	4
6	Serum albumin	P02768	69.4	5.92	3.94	2
7	Serotransferrin	P02787	77.1	6.81	3.72	2
8	Neurofilament triplet L protein	P07196	61.4	4.64	23.99	13
9	Calreticulin	P27797	48.1	4.29	15.59	6
10	Protein disulfide-isomerase	P07237	57.1	4.76	5.12	2
11	60 kDa heat shock protein, mitochondrial	P10809	61.1	5.7	15.36	8
11	Pyruvate kinase, isozymes M1/M2	P14618	57.8	7.95	3.58	2
12	Vimentin	P08670	53.5	5.06	39.57	15
13	Vacuolar ATP synthase subunit B, brain isoform	P21281	56.5	5.57	5.09	2
14	Vacuolar ATP synthase subunit B, brain isoform	P21281	56.5	5.57	7.24	3
15	Tubulin alpha-3 chain	Q71U36	50.1	4.94	17.29	7
15	Tubulin alpha-1 chain	P68366	49.9	4.95	14.96	6
16	S-arrestin	P10523	45.1	6.14	3.7	1
17	S-arrestin	P10523	45.1	6.14	19.01	7
18	S-arrestin	P10523	45.1	6.14	22.96	8
19	Tubulin beta-2C chain	P68371	49.8	4.79	19.55	8
19	Tubulin beta-2 chain	P07437	49.7	4.78	18.92	8
19	Tubulin beta-3 chain	Q13509	50.4	4.83	16.89	7
19	Tubulin beta-6 chain	Q9BUF5	49.9	4.77	11.88	5
20	ATP synthase beta chain, mitochondrial	P06576	56.6	5.26	25.9	8
21	Gamma-enolase	P09104	47.1	4.91	12.47	5
22	Eukaryotic initiation factor 4A-II	Q14240	46.4	5.33	16.22	5
22	Eukaryotic initiation factor 4A-I	P60842	46.2	5.32	12.56	4
23	Alpha-enolase	P06733	47	6.99	31.41	9
24	Alpha-enolase	P06733	47	6.99	24.71	9
25	Alpha-enolase	P06733	47	6.99	14.32	6
26	Alpha-enolase	P06733	47	6.99	22.86	8
27	Actin, cytoplasmic 1	P60709	41.7	5.29	16.53	5
27	Actin, cytoplasmic 2	P63261	41.8	5.31	16.53	5
27	Actin, gamma-enteric smooth muscle	P63267	41.9	5.31	11.7	4
27	Actin, aortic smooth muscle	P62736	42	5.24	11.67	4
28	Creatine kinase B-type	P12277	42.6	5.34	14.17	4
29	Glutamine synthetase	P15104	41.9	6.42	6.45	3
30	Glutamine synthetase	P15104	41.9	6.42	24.73	8
31	Glutamine synthetase	P15104	41.9	6.42	6.45	2
32	L-lactate dehydrogenase B chain	P07195	36.5	5.72	7.51	2
33	L-lactate dehydrogenase B chain	P07195	36.5	5.72	27.03	7
34	L-lactate dehydrogenase B chain	P07195	36.5	5.72	39.04	11
35	Cellular retinaldehyde-binding protein	P12271	36.3	4.98	22.15	6
36	Inorganic pyrophosphatase	Q15181	32.7	5.54	11.76	3
36	Guanine nucleotide-binding protein G(I)/G(S)/G(T) beta subunit 1	P62873	37.2	5.6	6.49	2
37	Inorganic pyrophosphatase	Q15181	32.7	5.54	14.88	4
37	Guanine nucleotide-binding protein G(I)/G(S)/G(T) beta subunit 1	P62873	37.2	5.6	11.5	4
38	Malate dehydrogenase, mitochondrial	P40926	35.5	8.92	19.82	6
38	Glyceraldehyde-3-phosphate dehydrogenase	P04406	35.9	8.58	10.78	3
39	14-3-3 protein epsilon	P62258	29.2	4.63	14.51	3
40	14-3-3 protein zeta/delta	P63104	27.7	4.73	14.69	3
40	14-3-3 protein theta	P27348	27.8	4.68	14.69	3
40	14-3-3 protein gamma	P61981	28.2	4.8	13.82	3
41	Recoverin	P35243	23	5.06	10.05	2
42	ATP synthase delta chain, mitochondrial	P30049	17.5	5.38	5.36	1
43	Alpha crystallin A chain	P02489	19.9	5.77	16.76	3
44	Hemoglobin beta subunit	P68871	15.9	6.81	22.6	3
45	Hemoglobin beta subunit	P68871	15.9	6.81	22.6	3
46	Hemoglobin alpha subunit	P69905	15.1	8.73	23.4	3

[a]Spot numbers correspond to the numbers on gel images in Fig. 1 (Peripheral-Coomassie). [b]Accession No. corresponds to UniProtKB/Swiss-prot database. [c]MW and pI are theoretical scores.

Table 2. Proteins identified in 40 spots detected only in macular gels

Spot No.[a]	Protein name	Database accession No.[b]	MW (kDa)[c]	pI[c]	Sequence coverage (%)	No. of peptide
M1	Pyruvate kinase, isozymes M1/M2	P14618	32.7	4.69	18.11	8
M2	Tropomyosin 1 alpha chain	P09493	32.7	4.69	13.73	5
M2	Heterogeneous nuclear ribonucleoproteins C1/C2	P07910	33.7	4.95	16.67	4
M3	Transaldolase	P37837	37.5	6.36	16.62	5
M3	3'(2'),5'-bisphosphate nucleotidase 1	O95861	33.4	5.46	10.06	3
M4	Poly(rC)-binding protein 1	Q15365	37.5	6.66	16.85	5
M5	Crk-like protein	P46109	33.8	6.26	7.59	2
M6	Heterogeneous nuclear ribonucleoproteins A2/B1	P22626	37.4	8.97	4.53	1
M7	Heterogeneous nuclear ribonucleoproteins A2/B1	P22626	37.4	8.97	11.9	3
M8	Voltage-dependent anion-selective channel protein 2	P45880	38.1	6.32	9.8	3
M9	Voltage-dependent anion-selective channel protein 1	P21796	30.6	8.63	7.8	2
M10	Voltage-dependent anion-selective channel protein 1	P21796	30.6	8.63	15.6	3
M11	Endoplasmic reticulum protein ERp29	P30040	29	6.77	27.59	6
M12	Guanylate kinase	Q16774	21.6	6.11	13.27	2
M13	Guanylate kinase	Q16774	21.6	6.11	19.39	3
M14	Gamma-synuclein	O76070	13.3	4.97	12.6	1
M15	Fatty acid-binding protein, epidermal	Q01469	15	6.8	21.64	3
M16	Arrestin-C	P36575	42.8	5.53	14.95	4
M17	Arrestin-C	P36575	42.8	5.53	4.64	1
M18	Isocitrate dehydrogenase [NAD] subunit alpha	P50213	39.6	6.46	22.4	7
M18	Transaldolase	P37837	37.5	6.36	15.73	5
M19	Tropomyosin 1 alpha chain	P09493	32.7	4.69	14.79	3
M19	Heterogeneous nuclear ribonucleoproteins C1/C2	P07910	33.7	4.95	12.75	3
M20	Pyruvate dehydrogenase E1 component beta subunit	P11177	39.2	6.2	31.75	8
M21	Glucose-6-phosphate 1-dehydrogenase	P11413	59.1	6.44	5.84	3
M22	Glucose-6-phosphate 1-dehydrogenase	P11413	59.1	6.44	9.73	5
M23	Glucose-6-phosphate 1-dehydrogenase	P11413	59.1	6.44	12.65	6
M24	26S proteasome non-ATPase regulatory subunit 11	O00231	47.3	6.09	23.04	8
M25	Elongation factor Tu	P49411	49.5	7.26	10.62	4
M26	Elongation factor Tu	P49411	49.5	7.26	4.87	2
M27	Alpha-centractin	P61163	42.6	6.19	8.78	2
M28	Heterogeneous nuclear ribonucleoproteins C1/C2	P07910	33.7	4.95	16.01	4
M29	Heterogeneous nuclear ribonucleoproteins C1/C2	P07910	33.7	4.95	22.55	6
M30	Heterogeneous nuclear ribonucleoprotein H3	P31942	36.9	6.37	11.27	3
M31	Voltage-dependent anion-selective channel protein 1	P21796	30.6	8.63	19.5	4
M31	Esterase D	P10768	31.5	6.54	4.61	1
M32	Pyruvate kinase, isozymes M1/M2	P14618	57.8	7.95	33.21	14
M33	Pyruvate kinase, isozymes M1/M2	P14618	57.8	7.95	29.43	13
M34	Aspartate aminotransferase	P17174	46.1	6.57	8.74	3
M35	Heterogeneous nuclear ribonucleoproteins A2/B1	P22626	37.4	8.97	9.92	3
M36	Heterogeneous nuclear ribonucleoproteins A2/B1	P22626	37.4	8.97	9.92	3
M37	Heterogeneous nuclear ribonucleoproteins A2/B1	P22626	37.4	8.97	7.37	2
M38	Heterogeneous nuclear ribonucleoproteins A2/B1	P22626	37.4	8.97	7.37	2
M39	Phosphoglycerate mutase 1	P18669	28.7	6.75	8.3	2
M40	Superoxide dismutase [Mn]	P04179	24.7	8.35	10.36	2

[a]Spot ID corresponds to the numbers on gel images in Fig. 1 (Macula-SYPRO Ruby). [b]Accession No. corresponds to UniProtKB/Swiss-prot database. [c]MW and pI are theoretical scores.

in the choroidal layer more specifically, sections were labeled with anti-PECAM1 antibody (Fig. 3H). PECAM1 is an adhesion molecule expressed at intercellular junctions between vascular endothelial cells [24] (Fig. 3J and 3K, green). Tropomyosin detected by TM311 (red) was expressed adjacent to PECAM1 (Fig. 3I and 3K).

Discussion

In this study, we identified and validated of proteins expressed in the macula and peripheral retina. The method, 2D gel electrophoresis, limits detection to proteins in aqueous soluble form. Nevertheless, a number

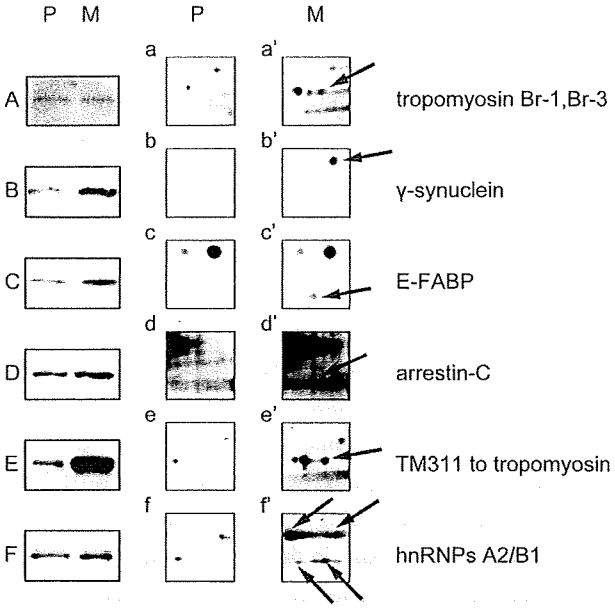

of proteins highly expressed in the macula were found.

One of the identified proteins was arrestin-C, which is known to be highly expressed in cone photoreceptors, which are densely located in the primate macula [6]. Previous SAGE analyses of the retina by Bowes Rickman *et al.* [3] have shown 1.4-fold higher transcription of arrestin-C in the macula compared to the peripheral

Fig. 2. Western blot of 5 proteins. Five micrograms of each sample from the peripheral retina and macula were loaded onto SDS-page gel (for γ-synuclein, 15 μg loading). After transferring to a PVDF membrane, the proteins were detected with antibodies specific to tropomyosin Br-1, Br-3 (A), γ-synuclein (B), E-FABP (C), arrestin-C (D), TM311 to tropomyosin (E), hnRNPs A2/B1 (F). Pieces of gel images (a–f, a'–f') correspond with the boxed areas in Fig. 1 (Peripheral-SYPRO Ruby and Macula-SYPRO Ruby). Lane P, peripheral retina; Lane M, macula.

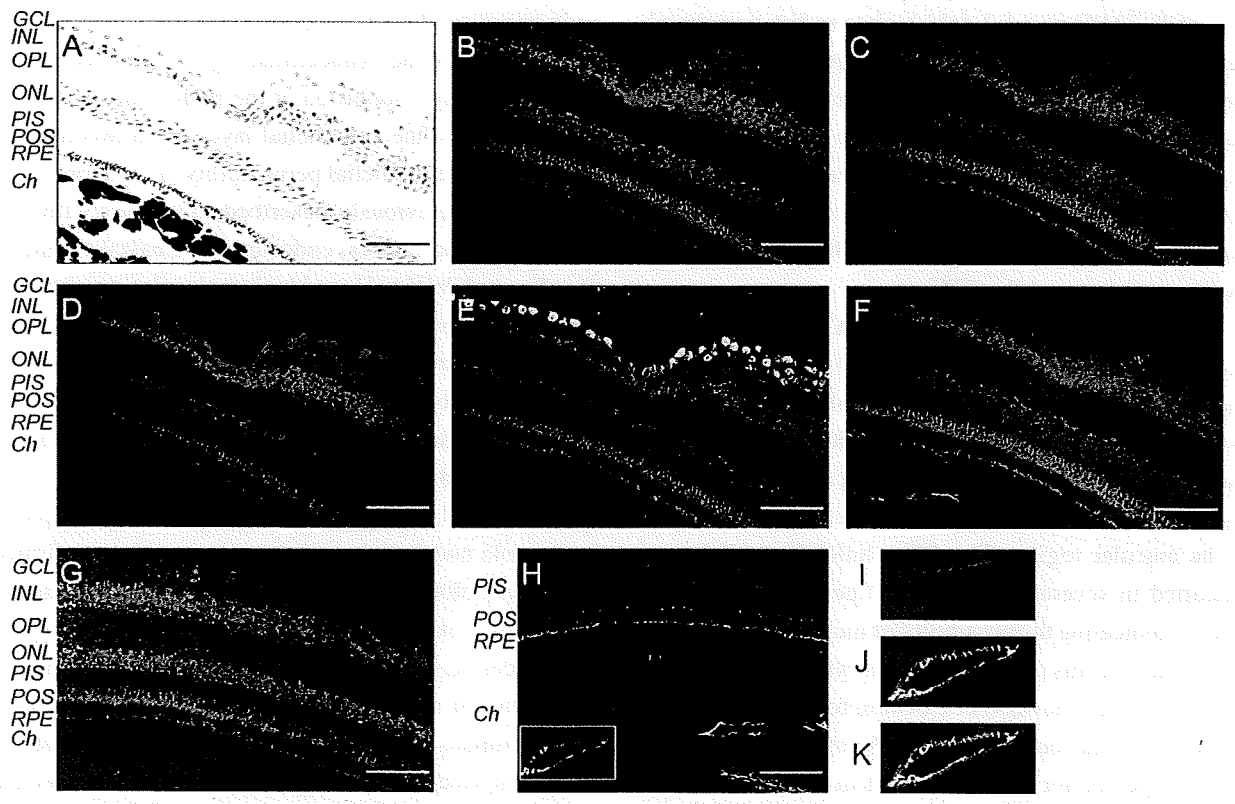

Fig. 3. Tissue localization of macula enriched proteins. Four-micrometer paraffin sections of monkey retina were stained with hematoxylin and eosin (A), other sections were labeled with antibodies specific to arrestin-C (B), tropomyosin Br-1, Br-3 (C), γ-synuclein (D), hnRNPs A2/B1 (E), TM311 to tropomyosin (F), and E-FABP (G). Tropomyosin was detected by TM311 in the choroidal layer (H). Boxed area in (H) is enlarged; labeled with antibodies specific to TM311 (red) (I), PECAM1 (green) (J), and merged (K). GCL, ganglion cell layer; INL, inner nuclear layer; OPL, outer plexiform layer; ONL, outer nuclear layer; PIS, photoreceptor inner segment; POS, photoreceptor outer segment; RPE, retinal pigment epithelial; Ch, choroid. (Bar; 50 μm)

retina in humans. Another protein that was identified in macular unique spots was 3'(2'),5'-bisphosphate nucleotidase 1 (Table 2, M3), which has also been identified by SAGE as being highly expressed in cone photoreceptors [3]. Identification of these cone photoreceptor rich proteins indicates that the present proteomic analysis was methodologically effective for identifying proteins richly expressed in the macula. It also suggests the higher protein level in the macula may be due to a higher density of specific cell types expressing specific proteins. Previous studies have shown arrestin-C expression in cones [33], γ-synuclein expression in RGCs [43], and E-FABP expression in Müller cells [21]. Although these proteins have been identified in not only specific cell types or compartments in the retina [1, 10, 15, 22, 50], the majority were localized in particular cell layers in the retina (Fig. 3B, 3D, and 3G). In a comparative transcription study of macular and peripheral RPE, expression of E-FABP was 6.3-fold higher in the peripheral RPE compared to macular RPE in middle-aged humans [48]. Our immunostaining showed predominant localization of E-FABP in the neural retina, except the photoreceptors (Fig. 3G), which is consistent with the results of Kingma *et al.* [21]. Our observation of higher E-FABP expression in the macula is due to higher expression by the neural retina, not the RPE.

Immunostaining revealed hnRNPs A2/B1 was present in every retinal nucleus layer (Fig. 3E). However, western blots showed higher expression of hnRNPs A2/B1 in the macula than in the peripheral retina (Fig. 2F). This may be explained by a higher concentration of RGC layers, where hnRNPs A2/B1 is preferentially expressed, in the macular region (Fig. 3E). hnRNPs A2/B1 was identified in several horizontal 2D gel spots (Fig. 1D, box. f') indicating the possibility of multiple phosphorylation sites for this protein. Phosphorylation of hnRNPs A2/B1 has been shown to be essential for the myelination of the axon-glia connection [51]. A similar myelination role is expected for hnRNPs A2/B1 in the RGCs.

In this study, two types of antibodies for tropomyosin isoforms were used. The brain-type isoform of tropomyosin detected by TMBr-3 antibody was not differentially expressed between the macula and peripheral retina (Fig. 2A), however tropomyosin detected by TM311 antibody showed remarkably higher expression in the macula (Fig. 2E). The difference in the expression level of the TM311-detected isoforms of tropomyosin resulted in an additional spot in the macula 2D gel which did not react with the TMBr-3 antibody. The TMBr-3-detected isoform is expressed in all regions of the brain [12, 41] and also in the outer plexiform layer and photoreceptor inner segments of the retina (Fig. 3C). This is in contrast to arrestin-C expression, which is limited to the photoreceptor outer segment (Fig. 3B). This is the first report to localize the brain-type isoform of tropomyosin in photoreceptors.

TM311 detected isoforms were localized to vascular endothelial cells compared to the localization of PECAM1 in choroid layer (Fig. 3H). Abundant expression of tropomyosin 1 α chain in the macula may arise from the higher capillary density in the choroidal layer of the fovea [30]. An earlier study, using human umbilical vein endothelial cells exposed to hydrogen peroxide, showed an increase in phosphorylation of tropomyosin through the activation of the extracellular signal-regulated kinase (ERK) pathway. Inhibition of the ERK pathway results in disruption of the endothelial layer and a two-fold increase in transendothelial permeability [17]. Tropomyosin has been previously described to interact with two anti-angiogenic factors, endostatin, a cleaved fragment of collagen XVIII [23], and high molecular weight kininogen [52]. Both proteins exhibit anti-angiogenic effect by binding to tropomyosin. Thus, tropomyosin may play an inhibitory role in increasing permeability or angiogenesis in the macula. Angiogenesis is a pathological finding often observed in the advanced stage of AMD [13].

In summary, 26 gel spots were identified as unique to the macula and 5 of these proteins were also confirmed by western blot as being richly expressed in the macula. Differential expression is likely due to morphological differences between the macula and the peripheral retina. The retina of macaque monkeys is almost identical to that of humans. Further understanding of these proteins should provide valuable information about the onset and progression of macular diseases in humans.

Acknowledgments

The authors thank Professor Duco Hamasaki for critical reading of the manuscript and helpful comments.

This study was funded in part by a grant to TI from the Ministry of Health, Labour and Welfare of Japan and by a grant to HO from the Ministry of Education, Culture, Sports, Science and Technology of Japan (KAKENHI 19791305).

References

1. Alge, C.S., Suppmann, S., Priglinger, S.G., Neubauer, A.S., May, C.A., Hauck, S., Welge-Lussen, U., Ueffing, M., and Kampik, A. 2003. Comparative proteome analysis of native differentiated and cultured dedifferentiated human RPE cells. *Invest. Ophthalmol. Vis. Sci.* 44: 3629–3641.
2. Bennaars-Eiden, A., Higgins, L., Hertzel, A.V., Kapphahn, R.J., Ferrington, D.A., and Bernlohr, D.A. 2002. Covalent modification of epithelial fatty acid-binding protein by 4-hydroxynonenal in vitro and in vivo. Evidence for a role in antioxidant biology. *J. Biol. Chem.* 277: 50693–50702.
3. Bowes Rickman, C., Ebright, J.N., Zavodni, Z.J., Yu, L., Wang, T., Daiger, S.P., Wistow, G., Boon, K., and Hauser, M.A. 2006. Defining the human macula transcriptome and candidate retinal disease genes using EyeSAGE. *Invest. Ophthalmol. Vis. Sci.* 47: 2305–2316.
4. Butt, R.H., Pfeifer, T.A., Delaney, A., Grigliatti, T.A., Tetzlaff, W.G., and Coorssen, J.R. 2007. Enabling coupled quantitative genomics and proteomics analyses from rat spinal cord samples. *Mol. Cell. Proteomics* 6: 1574–1588.
5. Cavusoglu, N., Thierse, D., Mohand-Said, S., Chalmel, F., Poch, O., Van-Dorsselaer, A., Sahel, J.A., and Leveillard, T. 2003. Differential proteomic analysis of the mouse retina: the induction of crystallin proteins by retinal degeneration in the rd1 mouse. *Mol. Cell. Proteomics* 2: 494–505.
6. Curcio, C.A., Allen, K.A., Sloan, K.R., Lerea, C.L., Hurley, J.B., Klock, I.B., and Milam, A.H. 1991. Distribution and morphology of human cone photoreceptors stained with anti-blue opsin. *J. Comp. Neurol.* 312: 610–624.
7. Distler, C. and Dreher, Z. 1996. Glia cells of the monkey retina—II. Müller cells. *Vision Res.* 36: 2381–2394.
8. Dreyfuss, G., Kim, V.N., and Kataoka, N. 2002. Messenger-RNA-binding proteins and the messages they carry. *Nat. Rev. Mol. Cell. Biol.* 3: 195–205.
9. El-Mofty, A., Gouras, P., Eisner, G., and Balazs, E.A. 1978. Macular degeneration in rhesus monkey (Macaca mulatta). *Exp. Eye Res.* 27: 499–502.
10. Ethen, C.M., Reilly, C., Feng, X., Olsen, T.W., and Ferrington, D.A. 2006. The proteome of central and peripheral retina with progression of age-related macular degeneration. *Invest. Ophthalmol. Vis. Sci.* 47: 2280–2290.
11. Feller, S.M. 2001. Crk family adaptors-signalling complex formation and biological roles. *Oncogene* 20: 6348–6371.
12. Had, L., Faivre-Sarrailh, C., Legrand, C., Mery, J., Brugidou, J., and Rabie, A. 1994. Tropomyosin isoforms in rat neurons: the different developmental profiles and distributions of TM-4 and TMBr-3 are consistent with different functions. *J. Cell Sci.* 107: 2961–2973.
13. Haddad, S., Chen, C.A., Santangelo, S.L., and Seddon, J.M. 2006. The genetics of age-related macular degeneration: a review of progress to date. *Surv. Ophthalmol.* 51: 316–363.
14. Harwerth, R.S. and Smith, E.L. 3rd. 1985. Rhesus monkey as a model for normal vision of humans. *Am. J. Optom. Physiol. Opt.* 62: 633–641.
15. Hauck, S.M., Schoeffmann, S., Deeg, C.A., Gloeckner, C.J., Swiatek-de Lange, M., and Ueffing, M. 2005. Proteomic analysis of the porcine interphotoreceptor matrix. *Proteomics* 5: 3623–3636.
16. Hope, G.M., Dawson, W.W., Engel, H.M., Ulshafer, R.J., Kessler, M.J., and Sherwood, M.B. 1992. A primate model for age related macular drusen. *Br. J. Ophthalmol.* 76: 11–16.
17. Houle, F., Rousseau, S., Morrice, N., Luc, M., Mongrain, S., Turner, C.E., Tanaka, S., Moreau, P., and Huot, J. 2003. Extracellular signal-regulated kinase mediates phosphorylation of tropomyosin-1 to promote cytoskeleton remodeling in response to oxidative stress: impact on membrane blebbing. *Mol. Biol. Cell* 14: 1418–1432.
18. Ishibashi, K., Tian, J., and Handa, J.T. 2004. Similarity of mRNA phenotypes of morphologically normal macular and peripheral retinal pigment epithelial cells in older human eyes. *Invest. Ophthalmol. Vis. Sci.* 45: 3291–3301.
19. Ishibashi, T., Sorgente, N., Patterson, R., and Ryan, S.J. 1986. Pathogenesis of drusen in the primate. *Invest. Ophthalmol. Vis. Sci.* 27: 184–193.
20. Ji, H., Liu, Y.E., Jia, T., Wang, M., Liu, J., Xiao, G., Joseph, B.K., Rosen, C., and Shi, Y.E. 1997. Identification of a breast cancer-specific gene, BCSG1, by direct differential cDNA sequencing. *Cancer Res.* 57: 759–764.
21. Kingma, P.B., Bok, D., and Ong, D.E. 1998. Bovine epidermal fatty acid-binding protein: determination of ligand specificity and cellular localization in retina and testis. *Biochemistry (Mosc)* 37: 3250–3257.
22. Liu, Q., Tan, G., Levenkova, N., Li, T., Pugh, E.N. Jr., Rux, J.J., Speicher, D.W., and Pierce, E.A. 2007. The proteome of the mouse photoreceptor sensory cilium complex. *Mol. Cell. Proteomics* 6: 1299–1317.
23. MacDonald, N.J., Shivers, W.Y., Narum, D.L., Plum, S.M., Wingard, J.N., Fuhrmann, S.R., Liang, H., Holland-Linn, J., Chen, D.H., and Sim, B.K. 2001. Endostatin binds tropomyosin. A potential modulator of the antitumor activity of endostatin. *J. Biol. Chem.* 276: 25190–25196.
24. Matsubara, T.A., Murata, T.A., Wu, G.S., Barron, E.A., and Rao, N.A. 2000. Isolation and culture of rat retinal microvessel endothelial cells using magnetic beads coated with antibodies to PECAM-1. *Curr. Eye Res.* 20: 1–7.
25. Monaco, W.A. and Wormington, C.M. 1990. The rhesus monkey as an animal model for age-related maculopathy. *Optom. Vis. Sci.* 67: 532–537.
26. Nicolas, M.G., Fujiki, K., Murayama, K., Suzuki, M.T., Mineki, R., Hayakawa, M., Yoshikawa, Y., Cho, F., and Kanai, A. 1996. Studies on the mechanism of early onset macular degeneration in cynomolgus (*Macaca fascicularis*) monkeys. I. Abnormal concentrations of two proteins in the retina. *Exp. Eye Res.* 62: 211–219.

27. Nicolas, M.G., Fujiki, K., Murayama, K., Suzuki, M.T., Shindo, N., Hotta, Y., Iwata, F., Fujimura, T., Yoshikawa, Y., Cho, F., and Kanai, A. 1996. Studies on the mechanism of early onset macular degeneration in cynomolgus monkeys. II. Suppression of metallothionein synthesis in the retina in oxidative stress. *Exp. Eye Res.* 62: 399–408.
28. Nishizawa, Y., Komori, N., Usukura, J., Jackson, K.W., Tobin, S.L., and Matsumoto, H. 1999. Initiating ocular proteomics for cataloging bovine retinal proteins: microanalytical techniques permit the identification of proteins derived from a novel photoreceptor preparation. *Exp. Eye Res.* 69: 195–212.
29. Ordya, J.M., Brizeea, K.R., and Hanscheb, J. 1980 Visual acuity and foveal cone density in the retina of the aged rhesus monkey. *Neurobiol. Aging* 1: 133–140.
30. Oyster, C.W. 1999. The Human Eye: Structure and Function, Sinauer Associates Inc., Massachusetts.
31. Provis, J.M., Penfold, P.L., Cornish, E.E., Sandercoe, T.M., and Madigan, M.C. 2005. Anatomy and development of the macula: specialisation and the vulnerability to macular degeneration. *Clin. Exp. Optom.* 88: 269–281.
32. Radeke, M.J., Peterson, K.E., Johnson, L.V., and Anderson, D.H. 2007. Disease susceptibility of the human macula: differential gene transcription in the retinal pigmented epithelium/choroid. *Exp. Eye Res.* 85: 366–380.
33. Sakuma, H., Inana, G., Murakami, A., Higashide, T., and McLaren, M.J. 1996. Immunolocalization of X-arrestin in human cone photoreceptors. *FEBS Lett.* 382: 105–110.
34. Schevzov, G., Vrhovski, B., Bryce, N.S., Elmir, S., Qiu, M.R., O'Neill, G.M., Yang, N., Verrills, N.M., Kavallaris, M., and Gunning, P.W. 2005. Tissue-specific tropomyosin isoform composition. *J. Histochem. Cytochem.* 53: 557–570.
35. Sharon, D., Blackshaw, S., Cepko, C.L., and Dryja, T.P. 2002. Profile of the genes expressed in the human peripheral retina, macula, and retinal pigment epithelium determined through serial analysis of gene expression (SAGE). *Proc. Natl. Acad. Sci. U.S.A.* 99: 315–320.
36. Snodderly, D.M., Auran, J.D., and Delori, F.C. 1984. The macular pigment. II. Spatial distribution in primate retinas. *Invest. Ophthalmol. Vis. Sci.* 25: 674–685.
37. Snodderly, D.M., Brown, P.K., Delori, F.C., and Auran, J.D. 1984. The macular pigment. I. Absorbance spectra, localization, and discrimination from other yellow pigments in primate retinas. *Invest. Ophthalmol. Vis. Sci.* 25: 660–673.
38. Snodderly, D.M., Weinhaus, R.S., and Choi, J.C. 1992. Neural-vascular relationships in central retina of macaque monkeys (*Macaca fascicularis*). *J. Neurosci.* 12: 1169–1193.
39. Stafford, T.J. 1974. Maculopathy in an elderly sub-human primate. *Mod. Probl. Ophthalmol.* 12: 214–219.
40. Stafford, T.J., Anness, S.H., and Fine, B.S. 1984. Spontaneous degenerative maculopathy in the monkey. *Ophthalmology* 91: 513–521.
41. Stamm, S., Casper, D., Lees-Miller, J.P., and Helfman, D.M. 1993. Brain-specific tropomyosins TMBr-1 and TMBr-3 have distinct patterns of expression during development and in adult brain. *Proc. Natl. Acad. Sci. U.S.A.* 90: 9857–9861.
42. Sueoka, E., Goto, Y., Sueoka, N., Kai, Y., Kozu, T., and Fujiki, H. 1999. Heterogeneous nuclear ribonucleoprotein B1 as a new marker of early detection for human lung cancers. *Cancer Res.* 59: 1404–1407.
43. Surguchov, A., McMahan, B., Masliah, E., and Surgucheva, I. 2001. Synucleins in ocular tissues. *J. Neurosci. Res.* 65: 68–77.
44. Suzuki, M.T., Terao, K., and Yoshikawa, Y. 2003. Familial early onset macular degeneration in cynomolgus monkeys (*Macaca fascicularis*). *Primates* 44: 291–294.
45. Umeda, S., Ayyagari, R., Allikmets, R., Suzuki, M.T., Karoukis, A.J., Ambasudhan, R., Zernant, J., Okamoto, H., Ono, F., Terao, K., Mizota, A., Yoshikawa, Y., Tanaka, Y., and Iwata, T. 2005. Early-onset macular degeneration with drusen in a cynomolgus monkey (*Macaca fascicularis*) pedigree: exclusion of 13 candidate genes and loci. *Invest. Ophthalmol. Vis. Sci.* 46: 683–691.
46. Umeda, S., Ayyagari, R., Suzuki, M.T., Ono, F., Iwata, F., Fujiki, K., Kanai, A., Takada, Y., Yoshikawa, Y., Tanaka, Y., and Iwata, T. 2003. Molecular cloning of ELOVL4 gene from cynomolgus monkey (*Macaca fascicularis*). *Exp. Anim.* 52: 129–135.
47. Umeda, S., Suzuki, M.T., Okamoto, H., Ono, F., Mizota, A., Terao, K., Yoshikawa, Y., Tanaka, Y., and Iwata, T. 2005. Molecular composition of drusen and possible involvement of anti-retinal autoimmunity in two different forms of macular degeneration in cynomolgus monkey (*Macaca fascicularis*). *FASEB J.* 19: 1683–1685.
48. van Soest, S.S., de Wit, G.M., Essing, A.H., ten Brink, J.B., Kamphuis, W., de Jong, P.T., and Bergen, A.A. 2007. Comparison of human retinal pigment epithelium gene expression in macula and periphery highlights potential topographic differences in Bruch's membrane. *Mol. Vis.* 13: 1608–1617.
49. Wang, Y.D., Wu, J.D., Jiang, Z.L., Wang, Y.B., Wang, X.H., Liu, C., and Tong, M.Q. 2007. Comparative proteome analysis of neural retinas from type 2 diabetic rats by two-dimensional electrophoresis. *Curr. Eye Res.* 32: 891–901.
50. West, K.A., Yan, L., Shadrach, K., Sun, J., Hasan, A., Miyagi, M., Crabb, J.S., Hollyfield, J.G., Marmorstein, A.D., and Crabb, J.W. 2003. Protein database, human retinal pigment epithelium. *Mol. Cell. Proteomics* 2: 37–49.
51. White, R., Gonsior, C., Kramer-Albers, E.M., Stohr, N., Huttelmaier, S., and Trotter, J. 2008. Activation of oligodendroglial Fyn kinase enhances translation of mRNAs transported in hnRNP A2-dependent RNA granules. *J. Cell Biol.* 181: 579–586.
52. Zhang, J.C., Donate, F., Qi, X., Ziats, N.P., Juarez, J.C., Mazar, A.P., Pang, Y.P., and McCrae, K.R. 2002. The antiangiogenic activity of cleaved high molecular weight kininogen is mediated through binding to endothelial cell tropomyosin. *Proc. Natl. Acad. Sci. U.S.A.* 99: 12224–12229.

j ocul biol dis inform (2009) 2:164–175
DOI 10.1007/s12177-009-9047-1

Genetic analysis of typical wet-type age-related macular degeneration and polypoidal choroidal vasculopathy in Japanese population

Asako Goto · Masakazu Akahori · Haru Okamoto · Masayoshi Minami · Naoki Terauchi · Yuji Haruhata · Minoru Obazawa · Toru Noda · Miki Honda · Atsushi Mizota · Minoru Tanaka · Takaaki Hayashi · Masaki Tanito · Naoko Ogata · Takeshi Iwata

Received: 12 September 2009 / Accepted: 6 November 2009 / Published online: 22 December 2009

Abstract Age-related macular degeneration (AMD) is a common cause of blindness in the elderly. Caucasian patients are predominantly affected by the dry form of AMD, whereas Japanese patients have predominantly the wet form of AMD and/or polypoidal choroidal vasculopathy (PCV). Although genetic association in the 10q26 (*ARMS2/HTRA1*) region has been established in many ethnic groups for dry-type AMD, typical wet-type AMD, and PCV, the contribution of the 1q32 (*CFH*) region seem to differ among these groups. Here we show a single nucleotide polymorphism (SNP) in the *ARMS2/HTRA1* locus is associated in the whole genome for Japanese typical wet-type AMD (rs10490924: $p = 4.1 \times 10^{-14}$, OR=4.16) and PCV (rs10490924: $p = 3.7 \times 10^{-8}$, OR=2.72) followed by *CFH* (rs800292: $p = 7.4 \times 10^{-5}$, OR=2.08; $p = 2.6 \times 10^{-4}$, OR=2.00), which differs from previous studies in Caucasian populations. Moreover, a SNP (rs2241394) in complement component *C3* gene showed significant association with PCV ($p = 2.5 \times 10^{-3}$, OR=3.47). We conclude that dry-type AMD, typical wet-type AMD, and PCV have both common

The first two authors Goto and Akahori have contributed equally to this work.

Electronic supplementary material The online version of this article (doi:10.1007/s12177-009-9047-1) contains supplementary material, which is available to authorized users.

A. Goto · M. Akahori · H. Okamoto · M. Minami · M. Obazawa · T. Iwata (✉)
Division of Molecular and Cellular Biology,
National Institute of Sensory Organs,
National Hospital Organization Tokyo Medical Center,
2-5-1 Higashigaoka,
Meguro-ku, Tokyo 152-8902, Japan
e-mail: iwatatakeshi@kankakuki.go.jp

N. Terauchi · Y. Haruhata · M. Obazawa · T. Noda
Division of Ophthalmology,
National Hospital Organization Tokyo Medical Center,
2-5-1 Higashigaoka,
Meguro-ku, Tokyo 152-8902, Japan

M. Honda · A. Mizota · M. Tanaka
Department of Ophthalmology,
Juntendo University Urayasu Hospital,
2-1-1, Tomioka,
Urayasu 279-0021, Japan

A. Mizota
Department of Ophthalmology, Teikyo University,
2-11-1, Kaga,
Itabashi-ku, Tokyo 173-8605, Japan

T. Hayashi
Department of Ophthalmology,
The Jikei University School of Medicine,
3-25-8, Nishi-shimbashi,
Minato-ku, Tokyo 105-8461, Japan

M. Tanito
Department of Ophthalmology,
Shimane University Faculty of Medicine,
Enya 89-1,
Izumo, Shimane 693-8501, Japan

N. Ogata
Department of Ophthalmology,
Kansai Medical University,
10-15, Fumizono-cho,
Moriguchi 570-0074, Japan

and distinct genetic risks that become apparent when comparing Japanese versus Caucasian populations.

Keywords Age-related macular degeneration · Polypoidal choroidal vasculopathy · ARMS2 · HTRA1 · CFH · C3

Introduction

Age-related macular degeneration (AMD) is the most common cause of blindness in elderly people of European descent and affects more than 1.75 million individuals in the USA alone [1]. In Japan, the prevalence of AMD has risen from 0.87% in 1988 to 1.3% in 2003 (Japan Ophthalmologists Association Study Group Report 2006–2008). Steady increase of AMD due to longer life span and improvement of diagnostic methods has been observed around the country. The most recent report by Kawasaki et al. describes the prevalence of early stage AMD in the Funagata study (Funagata-cho, Yamagata Prefecture, Japan) as 4.4% while the prevalence of late stage AMD was 1.1%, showing no difference from a Caucasian study in Australia [2].

AMD is considered a multifactorial disease with involvement of genetic, behavior, and environmental factors, and primarily affects the macular region of the retina [3]. Clinical phenotypes of AMD are manifold. Small and hard drusen often appear in normal-aged eyes and do not necessarily cause AMD [4]. In Caucasians, the early stage of AMD is associated with an increase in the number of large soft drusen and progresses to either the dry form or wet form of the disease [3]. In contrast, Japanese patients predominantly exhibit wet-type AMD with choroidal neovascularization and few or no drusen [5]. Maruko et al. have classified wet-type AMD patients into three subgroups, namely typical wet-type AMD, polypoidal choroidal vasculopathy (PCV), and retinal angiomatous proliferation (RAP) [5]. From 289 Japanese patients examined with wet-type AMD, 35.3%, 54.7%, and 4.5% were diagnosed with typical AMD, PCV, and RAP, respectively. In the remaining 5.5% patients, one eye had PCV and the other eye had typical AMD. Thus, PCV is the predominant subgroup of wet-type AMD in the Japanese population. PCV is characterized by branching of the choroidal vasculature basal to the RPE comprising various sized polypoidal structures connected to the branching vascular network, which can be clearly seen by indocyanine green angiography [6]. PCV can be misdiagnosed as typical AMD if only fluorescein angiography is performed. The recent increase in prevalence of PCV is mainly due to the improvement of diagnostic methods. In most Japanese patients, typical wet-type AMD and PCV occur unilaterally (94.1% and 81.6%, respectively) and show a male preponderance (71.6% and 77.8%, respectively) [5] consistent with studies of Eastern Asian patients in China and Korea [7, 8]. However, in Caucasians, PCV predominantly affects women and occurs bilaterally with a prevalence ranging from 4% to 14%, which is comparably lower than the Eastern Asian populations [6]. On the other hand, it has been reported that the incidence of PCV in black individuals exceeds that of Asians [6]. Although the phenotypic diversity of AMD has been speculated to be associated with differences in genetic background, this has not been clearly established.

Initial efforts to investigate the genetic basis of AMD utilized family studies. A concordance for AMD phenotypes in twins, and a higher risk of siblings of individuals with AMD have been reported [9–14]. These early studies lead to genome-wide linkage analyses using microsatellite markers to search for chromosomal regions associated with affected individuals [15–24]. Several candidate regions including 1q32 and 10q26 were confirmed by a meta-analysis [25]. Progress in genotyping and sequencing technology extended detailed genetic association studies to the entire genome. Age-related eye disease studies (AREDS) of AMD case-control subjects using 100,000 SNPs resulted in the identification of four chromosomal regions significantly associated with the disease, namely *CFH* (1q32), *ARMS2/HTRA1* (10q26), complement component 2/complement factor B (*C2/BF*, 6p21), and complement component 3 (*C3*, 19p13) [26], which is consistent with another genome wide association study recently reported by Swaroop et al. (*IOVS* 2009; 50:ARVO E-Abstract 1614). It should be noted that these genome-wide scans have been conducted on subjects with both the dry and wet form of AMD, with the majority of cases representing the dry form of the disease. However, Zang et al. have identified 34 SNPs which were associated with AMD at p value of less than 10^{-6} in the AREDS Caucasian cohort having typical wet-type AMD [27]. They showed that 1q32 and 10q26 were also significantly associated with typical wet-type AMD. To date, there are no genome-wide genetic studies reported for PCV.

Direct examinations of SNPs in chromosomal regions identified by genome-wide linkage analysis showed that two genomic loci 1q32 and 10q26 including the *CFH*, *ARMS2*, and *HTRA1* genes were associated with AMD in Caucasians and individuals of Hong Kong [28–32]. The association between AMD and three SNPs in these gene regions, namely rs1061170 (*CFH*), rs10490924 (*ARMS2*), and rs11200638 (*HTRA1*), were verified by a number of research groups around the world. We also confirmed the association of rs10490924 and rs11200638 with typical wet-type AMD in the Japanese cohort [33]. From our results and others, rs10490924 and rs11200638 have been shown to strongly associate with dry-type AMD [34], typical wet-type AMD [31, 32, 34], and PCV [35]. It is still unclear how these SNPs contribute to the development of

different types of AMD. On the other hand, no association was confirmed for rs1061170 in Japanese AMD [36–40]. This is probably due to the lower allele frequency of 0.07± 0.02 for this variant in Eastern Asian population compared to the higher frequency of 0.34±0.03 in Caucasians [41]. However, rs800292, another coding SNP in the *CFH* gene region originally associated with AMD in Caucasians [28], has been shown to associate with typical wet-type AMD and PCV in Japanese and Chinese populations [39, 42–44]. Thus, there is a clear difference in genetic risk for AMD based on ethnicity.

Since the association between the *CFH* gene and AMD has been established, other components of the complement pathway have been thoroughly examined in Caucasian populations. Among them, the 19p13, 6p21 and 4q25 loci, including the *C2*, *BF*, *C3*, and complement factor I (*CFI*) genes, show strong association with AMD [45–49]. However, it still unclear whether *CFI* or the nearby *PLA2G12A* gene is associated with the disease. Lee et al. analyzed the same AMD associated SNPs in the C2/BF gene region and reported that there were no differences between Chinese PCV patients and control groups [43]. Similar results were obtained for PCV in Japanese population for SNPs in the *C2/BF* gene region [50]. However, in this study, significant association of disease-protective haplotype was observed. There is currently no evidence that the *C2/BF* gene region is a risk for wet-type AMD or the *C3* gene region a risk for typical wet-type AMD and PCV for Eastern Asians. With the exception of 1q32, 10q26, 19p13, 6p21, and 4q25 regions, association of other loci with AMD pathogenesis reported by some genome-wide genetic studies remains unclear [15–24]. These SNP variants may be ethnic specific as is the case for *CFH*.

To investigate the involvement of genetic factors in Japanese patients who progressed to typical wet-type AMD and PCV, over 500,568 SNPs covering *ARMS2/HTRA1*, *CFH*, *C2/BF*, *C3*, and *CFI* and other regions were genotyped using Affymetrix Human Mapping 500 K Arrays and *Taq*Man assay.

Materials and methods

Subjects

One hundred Japanese patients with typical wet-type AMD but without PCV (average age 74.56±8.83 years), classified as 5b by Seddon et al. [51], 100 Japanese patients with PCV (average age, 72.71±8.25 years), and 190 age-matched Japanese controls (average age, 72.22±8.51 years) were recruited for this study (Table 1). All patients were diagnosed by ophthalmoscopic, fluorescein, and indocyanine green angiographic findings. In controls, no signs of early AMD, such as soft drusen or alterations of the retinal pigment epithelium in the macula area, were observed ophthalmoscopically. Informed consent was obtained from all participants and the procedures used conformed to the tenets of the Declaration of Helsinki.

Table 1 Summary of study populations

	AMD	PCV	Control	*p* value
No. of subjects	100	100	190	
Male/female	73:27	81:19	86:104	5.0×10^{-10}
Mean ± SD	74.56±8.83	72.71±8.25	72.22±8.51	0.08
Range	51–90	52–89	50–89	

p values were obtained by Pearson's chi-square test (5.0×10^{-10}) and one-way ANOVA (0.08) among three groups

AMD typical wet-type AMD

Genotyping

DNA was extracted from blood samples using the Magtration System 8Lx (Precision System Science Co., Ltd., Tokyo, Japan), and 50 ng/μl samples were evaluated by gel electrophoresis. Genotyping was performed on the Affymetrix GeneChip® Human Mapping 500 K Array Set (Affymetrix Japan, Tokyo, Japan), according to the manufacturer's instructions. To check the quality of each array, the SNPs were initially genotyped by a DM algorithm using Genotyping Console (Affymetrix). All arrays passed a call rate of 93% at a confidence threshold of 0.33. For the association analysis, we genotyped the SNPs by the Bayesian robust linear model with a Mahalanobis distance classifier (BRLMM) algorithm using Affymetrix Power Tools ver.1.10.0 (Affymetrix). Genotyping using Taqman® SNP Genotyping Assays (Applied Biosystems, Foster City, CA) on a StepOnePlus™ real-time PCR system (Applied Biosystems) was performed for the following SNPs in accordance with the manufacturer's instructions: rs800292, rs547154, rs2230199, rs10033900 (Assay ID: C_2530382_10, C_940286_10, C_26330755_10, C_34681305_10).

Statistical analyses

Statistical analyses were carried out with the R version of 2.7.0 [52]. Deviation of the genotype frequencies in the controls from those expected under Hardy-Weinberg Equilibrium (HWE) was assessed by chi-square test. SNPs with call rate <90% for case and control samples, respectively, a Hardy–Weinberg $p<0.0001$ for control samples, a minor allele frequency <0.05 for all samples, or those that exhibited poorly defined genotype clusters were disqualified from association analysis. For each case-control study, Fisher's exact test was used to compare allelic or genotypic